Journal of Molecular Structure 1074 (2014) 609–616

Contents lists available at ScienceDirect

Journal of Molecular Structure

journal homepage: www.elsevier.com/locate/molstruc

Crystal structures and theoretical calculations of two peculiar compounds derived from 4-benzoyl-3-methyl-1-phenyl-2-pyrazolin-5-one

Xingchen Yan [a,b,1], Xiaojing Wu [a,1], Jiakun Xu [a,c], Yuhua Fan [a,*], Caifeng Bi [a,*], Xia Zhang [a], Zhongyu Zhang [a]

[a] Key Laboratory of Marine Chemistry Theory and Technology, Ministry of Education, College of Chemistry and Chemical Engineering, Ocean University of China, Qingdao, Shandong 266100, PR China
[b] Qingdao Institute of Bioenergy and Bioprocess Technology, Chinese Academy of Sciences, Qingdao 266101, PR China
[c] Key Laboratory of Sustainable Development of Marine Fisheries, Ministry of Agriculture, Yellow Sea Fisheries Research Institute, Chinese Academy of Fishery Sciences, Qingdao 266071, PR China

HIGHLIGHTS

- Novel pyrazoline derivative potassium coordination polymer and organic salt.
- Various effects of coordination and intermolecular weak interactions was compared.
- Pyrazoline anions in the two compounds have the different conformations.
- The coplanarity of the two O atoms depends on their coordination environment.
- The sites for coordination and hydrogen bonding was predicted by calculations.

GRAPHICAL ABSTRACT

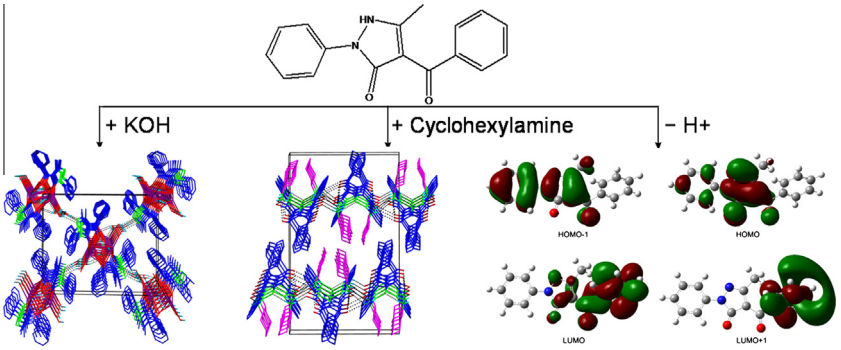

ARTICLE INFO

Article history:
Received 16 February 2014
Received in revised form 16 June 2014
Accepted 17 June 2014
Available online 22 June 2014

Keywords:
HPMBP derivative
Potassium coordination polymer
Crystal structure
Water cluster
Quantum chemistry calculation

ABSTRACT

A potassium coordination polymer $[K_2(PMBP)_2(H_2O)_3]_n{\cdot}2nH_2O$ (**1**) was prepared by reaction of 4-benzoyl-3-methyl-1-phenyl-2-pyrazolin-5-one (HPMBP) with potassium hydroxide. The single crystal of the supermolecule $C_6H_{11}NH_3^+{\cdot}PMBP^-$ (**2**) was then obtained by utilizing cyclohexylamine as the proton acceptor. It is a diketonate salt with an organic base where the $PMBP^-$ anions are stabilized by the intermolecular weak interactions (including hydrogen bonding, π–π stacking interactions and Van der Waals forces), rather than by coordination to a metal centre. Geometrical parameters of the isolated $PMBP^-$ anion were optimized through quantum chemistry calculation to simulate the state without any disturbances or interactions. Comparison of geometric parameters of compound **1** with the optimized structure of $PMBP^-$ provides an approach to study weak intermolecular interactions in the crystal state. The coordination sites and the proton acceptors of hydrogen bonds predicted by theoretical calculations are consistent to the experimental results.

Introduction

4-Acyl-5-pyrazolones derivatives have attracted intensive attentions during the past decades for their applications as analgesics, antipyretics, anti-inflammatory agents and insecticides [1]. Among

* Corresponding authors. Tel.: +86 0532 66781932.
E-mail addresses: fanyuhua301@163.com (Y. Fan), bicaifeng301@163.com (C. Bi).
[1] These authors contributed equally to the work.

http://dx.doi.org/10.1016/j.molstruc.2014.06.057
0022-2860/

these, 4-benzoyl-3-methyl-1-phenyl-2-pyrazolin-5-one (HPMBP) and its derivatives are widely utilized in the fields of trace metal separation [2–5], sterilization and deinsectization [6]. HPMBP has three potential coordination (donor) sites and may exist in four tautomers (Scheme 1) [7]. Crystal structures of tautomers **a** and **b** have been determined [8,9], but it is quite difficult to characterize the structure of its complexes due to the dramatic change of geometric parameters of the pyrazolone ring in the coordination process, which results from the deprotonation of HPMBP and rearrangement of the electron cloud of $PMBP^-$.

Although the transition metal complexes of HPMBP have been extensively studied [6,7,10–12], crystal structures of its alkali metal complexes have never been reported. Herein, we report a peculiar HPMBP potassium coordination polymer, $[K_2(PMBP)_2(H_2O)_3]_n{\cdot}2nH_2O$ (**1**). In the crystal structure, adjacent one-dimensional structures are connected into a three-dimensional network *via* five-membered water chains. Water chains are attracting a great deal of attentions because of their vital role in the biological transport of water, protons, and ions [13–15]. It was recently found that transport of water or protons across the cell involves the assembly of highly mobile hydrogen-bonded water molecules into a single chain at the positively charged constricted pore of the membrane-channel protein aquaporin-1 [16].

Supermolecular chemistry refers to the assembly of at least two molecules through spontaneous secondary interactions such as hydrogen bonding, dipole-dipole, charge transfer, Van der Waals, and π–π stacking interactions [17–21]. This so-called "bottom up" approach to construct nanostructures is advantageous over the "top down" approach such as microlithography which requires substantial effort to fabricate microstructures and devices as the target structures are extended to the range below 100 nm [22]. In addition, essential biological processes, such as signal transduction, biocatalysis, information storage, and processing, are all based on the supermolecular interactions between molecular components [23]. Thus, the single crystal of the supermolecule $C_6H_{11}NH_3^+{\cdot}PMBP^-$ (**2**) was obtained by employing cyclohexylamine as the proton acceptor. It is a diketonate salt with an organic base where the $PMBP^-$ anions are stabilized by the intermolecular weak interactions (including hydrogen bonding, π–π stacking interactions and Van der Waals forces), rather than by coordination to a metal centre. Geometric parameters of the isolated $PMBP^-$ anion were then optimized through quantum chemistry calculation to simulate the state without any disturbances or interactions. As a result, we are able to study the various effects of coordination and supermolecular interactions on the structure of $PMBP^-$ anion comparing geometries of compounds **1** and **2** with the optimized one. The quantum chemistry calculations can explain why the $PMBP^-$ anion coordinates to potassium, an element that is scarcely engaged in coordination.

Experimental

Materials and physical measurements

All reagents of analytical grade were used as obtained by commercial sources without further purification. Infrared spectra of the compounds were recorded in KBr pellets using a Nicolet 170SX spectrophotometer in the 4000–400 cm^{-1} region. ^1H NMR spectra were obtained on a Bruker DRX-600 spectrometer. Elemental analyses were carried out with a model 2400 Perkin–Elmer analyzer. X-ray diffraction data were collected on a Bruker Smart CCD X-ray single-crystal diffractometer.

*Synthesis of $[K_2(PMBP)_2(H_2O)_3]_n{\cdot}2nH_2O$ (**1**)*

A mixture containing L-Tyrosine (0.181 g, 1 mmol), KOH (0.056 g, 1 mmol) and methanol (30 mL) was stirred for 1 h at 60 °C. The obtained solution was filtered and HPMBP (0.278 g, 1 mmol) was added to the filtrate, which was further stirred for 4 h at 60 °C. The resulting solution was filtered and the filtrate was left at room temperature for slow evaporation in air. Colorless block crystals of compound **1** formed after approximately 30 days. ν_{max} (KBr)/cm^{-1}: 3111, 3354, 1624, 1593, 1578, 1497, 1456, 1431, 1397, 1352, 1062, 942, 838, 764, 698, 668, 657, 609. ^{1}HNMR (CD_3OD, 600 MHz) δ 7.74 (d, *J* 7.8, 2H, NC_6H_5), 7.66 (d, *J* 6.6, 2H, NC_6H_5), 7.39 (m, 5H, CC_6H_5), 7.13 (t, *J* 7.2, 1H, NC_6H_5), 2.27 (s, 3H, CH_3). Anal. Calc. for $C_{34}H_{36}K_2N_4O_9$: C 56.49, H 5.02, N 7.75. found: C 56.63, H 4.93, N 7.66%.

*Synthesis of $C_6H_{11}NH_3^+{\cdot}PMBP^-$ (**2**)*

A mixture containing HPMBP (0.278 g, 1 mmol), cyclohexylamine (0.099 g, 1 mmol) and methanol (30 mL) was stirred for 4 h at 60 °C. The resulting solution was filtered and the filtrate was left at room temperature for slow evaporation in air. Colorless block crystals of compound **2** formed after approximately 30 days. ν_{max} (KBr)/cm^{-1}: 2934, 2856, 1625, 1593, 1553, 1521, 1499, 1452, 1429, 1395, 1348, 944, 835, 769, 699, 610. ^{1}HNMR (CD_3OD, 600 MHz) δ 7.73 (d, *J* 7.8, 2H, NC_6H_5), 7.66 (d, *J* 6.6, 2H, NC_6H_5), 7.39 (m, 5H, CC_6H_5), 7.14 (t, *J* 7.2, 1H, NC_6H_5), 2.97 (m, 1H, $CHNH_3^+$), 2.29 (s, 3H, CH_3), 1.96 (d, *J* 10.8, 2H, CH_2), 1.80 (d, *J* 13.2, 2H, CH_2), 1.67 (d, *J* 13.2, 1H, CH_2), 1.32 (m, 4H, CH_2), 1.19 (m, 1H, CH_2). ^{1}HNMR (DMSO-d_6, 600 MHz) δ 8.03 (d, *J* 7.8, 2H, NC_6H_5), 7.72 (s, 3H, NH_3^+), 7.59 (d, *J* 6.6, 2H, NC_6H_5), 7.31 (m, 3H, CC_6H_5), 7.23 (t, *J* 7.8, 2H, CC_6H_5), 6.91 (t, *J* 7.2, 1H, NC_6H_5), 2.90 (m, 1H, $CHNH_3^+$), 2.19 (s, 3H, CH_3) 1.86 (s, 2H, CH_2), 1.69 (s, 2H, CH_2), 1.56 (d, *J* 12.6, 1H, CH_2), 1.22 (m, 4H, CH_2), 1.08 (m, 1H, CH_2). Anal. Calc. for $C_{23}H_{27}N_3O_2$: C 56.49, H 5.02, N 7.75; found: C 56.33, H 5.14, N 7.67%.

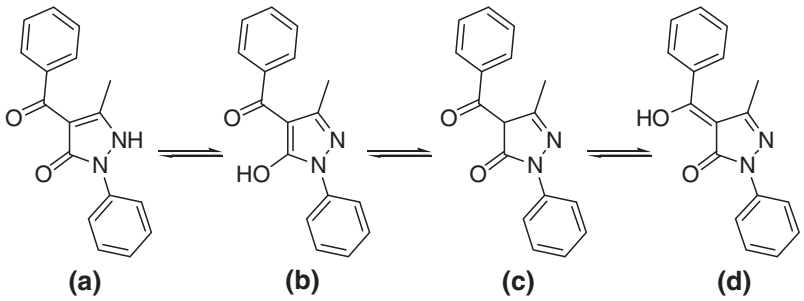

Scheme 1.

Crystallographic data collection and structure determination

Diffraction intensity data of single crystals of compounds **1** and **2** were collected on a Bruker Smart CCD X-ray single-crystal diffractometer equipped with a graphite monochromated Mo Kα radiation ($\lambda = 0.71073$ Å) by using a φ and ω scan mode at 298(2) K. The diffraction data were integrated by using the *SAINT* program [24]. Empirical absorption correction was applied using the *SADABS* programs [25]. The structures refinements were against F^2 by the full-matrix least-squares technique using the *SHELXTL* crystallographic software package [26]. All non-hydrogen atoms were found in the final difference Fourier map. Hydrogen atoms were fixed geometrically at calculated distances and allowed to ride on the parent non-hydrogen atoms. Positional and thermal parameters were refined by full-matrix least-squares method to convergence. The crystallographic data of compounds **1** and **2** are summarized in Table 1.

Computational details

Atom coordinates used in the calculations were from crystallographic data. A $PMBP^-$ anion in compound **2** was selected as the initial model for the isolated $PMBP^-$, and was optimized to find the stationary point. The calculations were carried out by Density Functional Theory (DFT) B3LYP method with 6-31+G* basis set. The harmonic vibrational frequencies were calculated at the same level of theory for the optimized $PMBP^-$. The vibrational frequency calculations revealed no imaginary frequencies, indicating that the stationary point at this level of approximation was found for $PMBP^-$. The molecular electrostatic potential, $V(\boldsymbol{r})$, at a given point $\boldsymbol{r}(x, y, z)$ in the vicinity of a molecule, is defined in terms of the interaction energy between the electrical charge generated by the molecule's electrons and nuclei and a positive test charge (a proton) located at $\boldsymbol{r}$. All calculations were conducted on a Pentium IV computer using *Gaussian 03* program [27]. The graphics of the optimized geometry, MEP maps and frontier molecular orbitals were generated using *GaussView 5.0.9* [28].

Table 1
The crystallographic data and structure refinement for compounds 1 and 2.

Compound	Compound **1**	Compound **2**
Empirical formula	$C_{34}H_{36}K_2N_4O_9$	$C_{23}H_{27}N_3O_2$
Formula weight	722.87	377.48
Temperature (K)	298(2)	298(2)
Wavelength (Å)	0.71073	0.71073
Crystal system	Monoclinic	Monoclinic
Space group	$P2_1/n$	$P2_1/c$
a (Å)	11.6364(9)	12.3456 (11)
b (Å)	16.1665(12)	14.4090 (13)
c (Å)	19.4938(17)	23.339 (2)
α (°)	90	90
β (°)	104.5630(10)	93.8800 (10)
γ (°)	90	90
Volume (Å^3)	3549.4(5)	4142.2 (7)
Z	4	8
Calculated density (g/cm^3)	1.353	1.211
Absorption coefficient (mm^{-1})	0.325	0.078
$F(000)$	1512	1616
Crystal size (mm)	0.49 × 0.40 × 0.36	0.18 × 0.16 × 0.13
θ range for data collection (°)	2.33 to 25.02	2.72 to 25.02
Limiting indices	$-13 \leqslant h \leqslant 10$ $-19 \leqslant k \leqslant 19$ $-23 \leqslant l \leqslant 21$	$-14 \leqslant h \leqslant 14$ $-17 \leqslant k \leqslant 17$ $-16 \leqslant l \leqslant 27$
Reflections collected/unique	17140/6257 [R_{int} = 0.0772]	20,720/7297 [R_{int} = 0.0990]
Completeness to θ = 25.02	0.998	0.998
Max. and min. transmission	0.8920 and 0.8570	0.9899 and 0.9861
Data/restraints/parameters	6257/0/444	7297/0/509
Goodness of fit on F^2	1.062	1.049
R_1[a], wR_2[b] [$I > 2\sigma(I)$]	R_1 = 0.0599, wR_2 = 0.1342	R_1 = 0.0595, wR_2 = 0.0869
R_1[a], wR_2[b] (all data)	R_1 = 0.1317, wR_2 = 0.1810	R_1 = 0.1919, wR_2 = 0.1009
Largest diff. peak and hole (e. Å^3)	0.394 and −0.403	0.468 and −0.340

[a] $R = \Sigma\,(||F_0|-|F_C||)/\Sigma\,F_0$.
[b] $wR = [\Sigma\,w(|F_0|^2-|F_C|^2)^2/\Sigma\,w(F_0^2)]^{1/2}$.

Results and discussions

*Crystal structure description of $[K_2(PMBP)_2(H_2O)_3]_n{\cdot}2nH_2O$ (**1**)*

Selected bond lengths and angles for compound **1** are listed in Table S1 in supplementary materials. Comparison of hydrogen bonding geometrical parameters for compounds **1** and **2** are listed in Table 2. As shown in Fig. 1a, compound **1** is a neutral coordination polymer, consisting of potassium cations and $PMBP^-$ anions connected by coordination bonds. The ligand containing O1A and O2A is designated as ligand **1A** while the ligand containing O1B and O2B is designated as ligand **1B**. There are coordinated (O1, O2, O3) and solvent (O4, O5) water molecules in the crystal lattice. K1 coordinates with six atoms. Among them, two are O1B and O2B in ligand **1B**, one is O1A in ligand **1A**, one is O1 from the coordinated water, and the other two are the atoms generated from O1B and O2B through symmetry operation (i) shown in Fig. 1a. K2 coordinates with five atoms. Among them, two are O1A and O2A in ligand **1A**, two are O2 and O3 from the coordinated water, and the other one is the atom generated from O2A through symmetry operation (ii) shown in Fig. 1a. There are two six-membered chelating rings around K1, namely ring K1—O1B—C1B—C2B—C5B—O2B—K1 and the ring generated from it through symmetry operation (i). Around K2, there is one six-membered chelating ring K2—O1A—C1A—C2A—C5A—O2A—K2.

As shown in Fig. 1b, O1B and O2B in ligand **1B** coordinate with K1 and the atom it generated through symmetry operation (i) at the same time. An octahedral cage is formed by six atoms, which are O1B, O2B, K1 and the atoms generated by them through symmetry operation (i). O2A in ligand **1A** coordinates with K2 and the atom generated from K2 through symmetry operation (ii) at the same time. A parallelogram ring is formed by four atoms, which are O2A, K2 and the atoms generated by them through symmetry operation (ii). In this way, a chain structure along the a axis is formed through coordination bonds.

As shown in Fig. 1c, adjacent chains lying parallel to each other are connected by water molecules *via* hydrogen bonds into three-dimensional network. Herein, a water chain: O2···H1A—O1—H1B···O4—H4B···O5—H5B···O3 is formed by these water molecules *via* hydrogen bonds (Fig. 1d). O3 is linked to O1A and O1B in one chain to give two intramolecular O—H···O hydrogen bonds, and O9 is linked to O2B to give an intermolecular O—H···O hydrogen bond. In contrast, O2 and O4 are linked to N2A and N2B in another chain to give two intermolecular O—H···N hydrogen bonds, respectively.

*Crystal structure description of $C_6H_{11}NH_3^+{\cdot}PMBP^-$ (**2**)*

Selected bond lengths and angles for compound **2** are listed in Table S2 in supplementary material. As shown in Fig. 2a, compound **2** is a supermolecule consisting of $PMBP^-$ anions and cyclohexylammonium cations. The asymmetric unit contains two independent cations and two independent anions. The anion containing O1A and O2A is designated as anion **2A** while the anion containing O1B and O2B is designated as anion **2B**. There exist π–π stacking interactions between the adjacent phenyl rings in

Table 2
Comparison of hydrogen bonding geometrical parameters for compounds **1** and **2** (Å, °).

	d(D—H)	*d*(H···A)	*d*(D···A)	<(D—H···A)
1				
O1—H1A···O2	0.85	2.17	2.903(6)	145.0
O1—H1B···O4[a]	0.85	2.05	2.747(6)	138.9
O2—H2A···N2A[b]	0.85	2.27	2.834(5)	124.2
O2—H2B···O1	0.85	2.22	2.903(6)	136.9
O3—H3A···O1A[c]	0.85	1.94	2.785(4)	176.7
O3—H3B···O1B[d]	0.85	1.90	2.747(4)	176.8
O4—H4A···N2B	0.85	2.04	2.887(5)	179.3
O4—H4B···O5[e]	0.85	1.96	2.812(7)	179.7
O5—H5A···O2B[f]	0.85	2.15	2.958(5)	160.1
O6—H5B···O3[g]	0.85	2.07	2.880(5)	160.0
2				
N1C—H1CA···O1A	0.8900	2.1200	2.888(4)	144.00
N1C—H1CA···O2A	0.8900	2.4900	3.127(4)	129.00
N1C—H1CB···N2A[h]	0.8900	2.1300	3.012(4)	169.00
N1C—H1CC···O1B[i]	0.8900	2.2300	3.112(4)	170.00
N1C—H1CC···O2B[i]	0.8900	2.4600	2.909(4)	111.00
N1D—H1DA···N2B[j]	0.8900	2.1300	3.005(4)	168.00
N1D—H1DB···O1B[i]	0.8900	1.9600	2.840(4)	169.00
N1D—H1DC···O1A	0.8900	2.0700	2.949(4)	168.00
N1D—H1DC···O2A	0.8900	2.5300	3.006(4)	114.00

[a] Symmetry code: $-x+3/2, y-1/2, -z+3/2$.
[b] Symmetry code: $-x+1/2, y-1/2, -z+3/2$.
[c] Symmetry code: $-x, -y+1, -z+1$.
[d] Symmetry code: $x-1, y, z$.
[e] Symmetry code: $-x+3/2, y+1/2, -z+3/2$.
[f] Symmetry code: $-x+1, -y+1, -z+1$.
[g] Symmetry code: $x+1, y, z$.
[h] Symmetry code: $-x+1, y+1/2, -z+1/2$.
[i] Symmetry code: x, y, z.
[j] Symmetry code: $-x+1, y-1/2, -z+1/2$.

ligands **1A** and **1B**. The distance between the centre of the two phenyl rings is 3.921(3) Å. Their dihedral angle is 4.3(2) Å, indicating that they are nearly parallel to each other. The slippage between them is 3.4374(18) Å, indicating that it is offset face-to-face π–π stacking interaction. $PMBP^-$ anions are connected by cyclohexylammonium cations *via* N—H···N and two bifurcated N—H···O hydrogen bonds, forming a chain structure along the *a* axis (Fig. 2b). Adjacent chains are further connected by N—H···O hydrogen bonding and bifurcated N—H···O hydrogen bonding into a two-dimensional network (Fig. 2c). As viewed along the *a* axis, the crystal is further stabilized by the Van der Waals forces to assemble a three-dimensional supermolecular structure (Fig. 2d). In most cases when such diketonate salt with ammonium cations were found in the solid state (CSD reference codes FAGPOS, VECKEU, VECKIY, XUZWIY and PINCUK), they participated in similar hydrogen bonding as in compound **2** [29–32]. They are comprised of acetylacetonate derivative anions and secondary ammonium cations. In these structures, one N—H bond in the secondary ammonium cation forms bifurcated N—H···O hydrogen bonding to two O atom acceptors in the diketonate anion, while the other N—H bond forms N—H···O hydrogen bonding to one of the O atom acceptor in another diketonate anion. In this way tetramers similar to existing in crystal structure of compound **2** (shown in the ellipse in Fig. 2c) are formed but in contrast they are connected only by van der Waals forces.

Characterization of the protonated cyclohexylamine

Limited by the quality of the single crystals, the hydrogen atoms were fixed geometrically at calculated distances and allowed to ride on the parent non-hydrogen atoms. However, the protonation of cyclohexylamine can be characterized by IR and ^{1}H NMR data. For IR data, the absorption maximum of compound **2** at 2934 cm^{-1} and 2356 cm^{-1} can be assigned to the antisymmetric stretch $\nu_{as}NH_3^+$, and the symmetric stretch $\nu_sNH_3^+$, whereas the antisymmetric and symmetric stretch bands of NH_2 should exist between 3500 cm^{-1} and 3300 cm^{-1}. This can prove the protonation of cyclohexylamine in the solid state. The ^{1}H NMR spectra were recorded in CD_3OD to characterize and compare the skeleton structures of the two compounds in solution. The signals in the range of 7.74–7.13 ppm are assigned to the resonance of the hydrogen atoms in the two phenyl rings. The chemical shifts around 2.27 ppm are assigned to the resonance of the hydrogen atoms in methyl. The corresponding chemical shifts and coupling constant are very similar in the two compounds. For compound **2**, there exists additional signals of 2.97 ppm and 1.96–1.19 ppm, which are assigned to the resonance of the hydrogen atoms in the cyclohexyl skeleton. The ^{1}H NMR spectrum recorded in CD_3OD can prove the coexistence of the HPMBP and cyclohexylamine in solution. To characterize the position of the reactive hydrogen atoms in solution, the ^{1}H NMR spectrum of compound **2** was recorded in DMSO-d_6. Apart from the assignments above, an additional signal appears at 7.72 ppm, which is assigned to the resonance of the hydrogen atoms in the protonated amino group, NH_3^+. In addition, no additional signals were found in the spectrum, indicating the deprotonation of HPMBP.

Comparison of the geometric parameters

The optimized geometry of $PMBP^-$ is shown in Fig. 3 to simulate the state without any disturbances or interactions. To study the various effects of coordination and intermolecular weak interactions on the structure of the $PMBP^-$ anion, structural comparison is made between ligands **1A**, **1B**, cations **2A**, **2B** and the optimized $PMBP^-$, which is listed in Table 3. All the values in the same row are their corresponding values. The geometric parameters used in the following comparisons and discussions are taken from the experimental data for compounds **1** and **2**, and from the calculated values for $PMBP^-$ after optimization.

For the optimized $PMBP^-$, O1, N1, N2, C1, C2, C3, C12, C13, C14, C15, C16 and C17 are nearly coplanar, indicating that the phenyl ring and the pyrazolone ring can form a large conjugated system. The large C1—C2—C5—O2 torsion angle of 20.0° and O···O separation of 3.086 Å are attributed to the electronic repulsion between O1 and O2. The large torsion angle of C2—C5—C6—C7 (49.6°) is attributed to the repulsion force between H7 and C4, because if the phenyl ring and the pyrazolone ring were coplanar, they would be overlapped.

For compound **1**, O1A, N1A, N2A, C1A, C2A, C3A and C5A are coplanar in ligand 1A. O1A coordinates with K1 and K2 simultaneously while O2A coordinates with two K2. This elongates C1A—O1A and increases the C1A—C2A—C5A—O2A torsion angle (25.2(6)°). As a result, O1A—C1A is approximately 0.032 Å longer than O2A—C5A in ligand **1A**, whereas the two O—C bond lengths are similar in the optimized $PMBP^-$. But the O···O separation has decreased (3.035(6) Å), because the coordinated potassium anions can decrease the repulsion force. In contrast, ligand **1B** has a more symmetric structure, because O1B and O2B coordinate to two K1 simultaneously to form two six-membered rings. As a result, the two O—C bonds still maintain the similar distance, and both O2A and O2B is coplanar with the pyrazolone ring. In addition, the O···O separation (2.915(6) Å) is smaller than that in ligand 1A. The corresponding phenyl rings in ligand **1A**, ligand **1B** and the optimized $PMBP^-$ have the different conformations, which is caused by the steric hindrance in compound **1**.

For compound **2**, O1A—C1A is approximately 0.026 Å longer than O2A—C5A in anion **2A**, and O1B—C1B is approximately 0.018 Å longer than O2B—C5B in anion **2B**. The C1A—C2A—C5A—O2A and C1B—C2B—C5B—O2B torsion angles of 14.9(6)° and −21.1(6)° are similar to that in $PMBP^-$, but they rotate

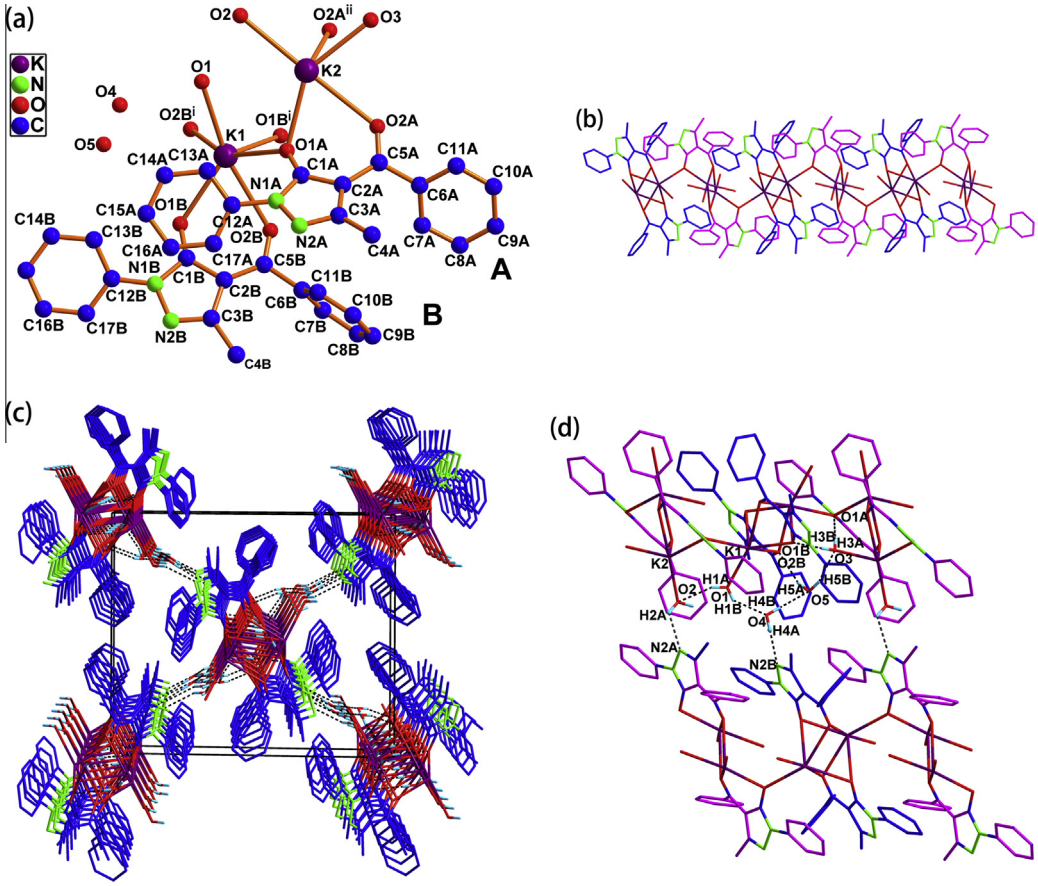

Fig. 1. (a) The atomic labeling scheme for an asymmetric unit of compound **1** (all hydrogen atoms are omitted for clarity), symmetry codes: (i) $-x+3$, $-y+1$, $-z+1$; (ii) $-x+2$, $-y+1$, $-z+1$; (b) the chain structure along the *a* axis in compound **1;** (c) the packing diagram of the unit cell of compound **1** viewed along the *a* axis; (d) view of the five-membered water chain in compound **1**.

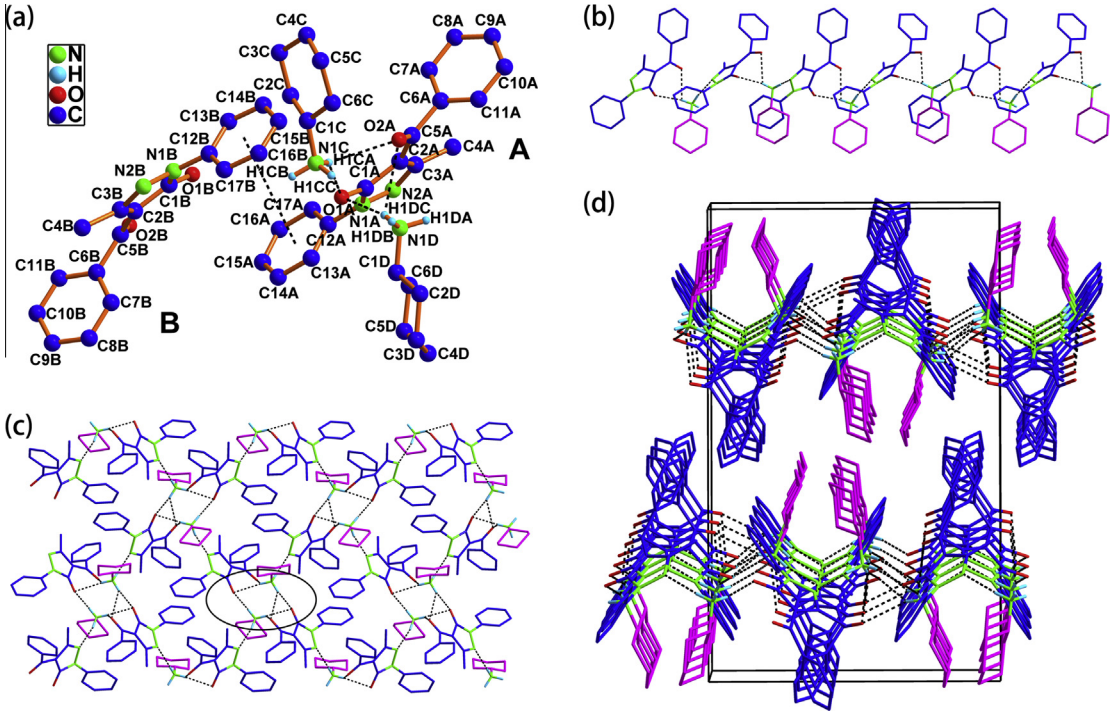

Fig. 2. (a) The atomic labeling scheme for an asymmetric unit of compound **2** (all hydrogen atoms are omitted for clarity, except for those in NH_3^+); (b) the chain structure along the *a* axis in compound **2**; (c) the two-dimensional network viewed along the *c* axis in compound **2**; (d) the packing diagram of the unit cell of compound **2** viewed along the *a* axis.

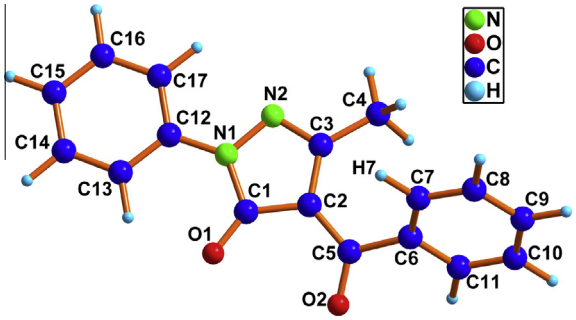

Fig. 3. The optimized molecular structure of $PMBP^-$.

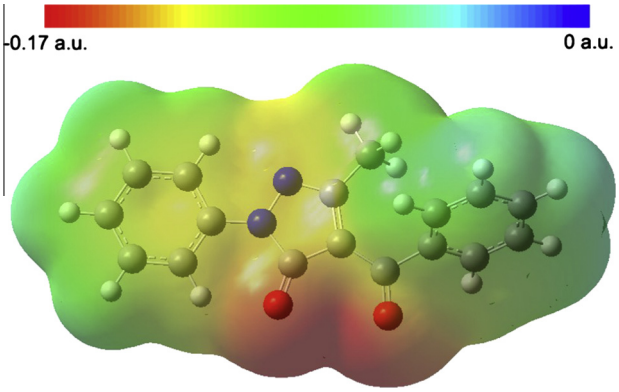

Fig. 4. The total electron density mapped with electrostatic potential surface of the optimized $PMBP^-$.

in different directions. This may be ascribed to the hydrogen bonding and electrostatic interactions between cyclohexylammonium cations and $PMBP^-$ anions. The phenyl rings consisting of C12A ~ C17A and C12B ~ C17B are designated as ring 1 ring 2, respectively. Both N1A—C12A and N1B—C12B are not coplanar with the pyrazolone rings, and ring 1 and ring 2 are parallel to each other. The large torsion angles of C1A—N1A—C12A—C13A (−56.3(6)°) and C1B—N1B—C12B—C13B (52.9(6)°), and the distortion of N—C bonds in anions **2A** and **2B** are attributed to the π–π stacking interaction between ring 1 and ring 2 (Fig. 2a). They must rotate along the N—C bonds to make the two phenyl rings parallel to decrease the distance between them. The corresponding phenyl rings in ligand **2A**, ligand **2B** and the optimized $PMBP^-$ have the different conformations, which should be also caused by the steric hindrance in compound **2**.

Quantum chemistry calculations

MEP is related to the electronic density and is a very useful descriptor in understanding sites for electrophilic attack and nucleophilic reactions as well as hydrogen bonding interactions [33]. The electrostatic potential $V(\boldsymbol{r})$ are also well suited for analyzing processes based on the 'recognition' of one molecule by another, as in drug-receptor, and enzyme-substrate interactions, because it is through their potentials that the two species first 'see' each other [34]. To predict reactive sites for coordination and hydrogen bonding for $PMBP^-$, MEP surface based on the optimized geometry was mapped on total electron density (Fig. 4).

As shown in Fig. 4, the MEP of the optimized $PMBP^-$ in the whole structure is negative, because the large delocalization extent caused the transfer to the whole structure of the negative charge brought by deprotonation. The most negative regions are found between O1 and O2 with the value of −0.201 a.u. (Fig. 3c). Due to the negative MEP in the whole structure and the more negative region between O1 and O2, $PMBP^-$ anion can chelate potassium or form bifurcated hydrogen bonds in the alkaline condition to stabilize the structure and neutralize the negative electronic potential. There is another negative region of the anion around N2 atom (−0.139 a.u.) which may attract hydrogen bond. This is consistent to the experimental results that O1, O2 and N2 are proton

Table 3
Comparison of the important bond lengths and torsion angles between the experimental data for compounds **1** and **2**, and the calculated values for the optimized $PMBP^-$ (Å, °).

Bond	**1A**	Bond	**1B**		
O1A—C1A	1.271(5)	O1B—C1B	1.257(5)		
O2A—C5A	1.239(5)	O2B—C5B	1.248(5)		
N1A—C1A	1.374(5)	N1B—C1B	1.394(5)		
N1A—N2A	1.395(4)	N1B—N2B	1.395(5)		
N2A—C3A	1.330(5)	N2B—C3B	1.307(5)		
C1A—C2A	1.426(6)	C1B—C2B	1.432(6)		
C2A—C3A	1.408(5)	C2B—C3B	1.435(6)		
C2A—C5A	1.447(6)	C2B—C5B	1.418(6)		
Torsion angle	**1A**	Torsion angle	**1B**		
C1A—N1A—C12A—C13A	−35.3(6)	C1B—N1B—C12B—C13B	−27.1(6)		
C1A—C2A—C5A—O2A	25.2(6)	C1B—C2B—C5B—O2B	−0.3(7)		
C3A—C2A—C5A—C6A	33.7(6)	C3B—C2B—C5B—C6B	−1.0(7)		
C2A—C5A—C6A—C7A	46.2(6)	C2B—C5B—C6B—C7B	−78.1(6)		
Bond	**2A**	Bond	**2B**	Bond	$PMBP^-$
O1A—C1A	1.268(4)	O1B—C1B	1.259(4)	O1—C1	1.238
O2A—C5A	1.242(4)	O2B—C5B	1.241(4)	O2—C5	1.243
N1A—C1A	1.378(4)	N1B—C1B	1.387(4)	N1—C1	1.430
N1A—N2A	1.399(4)	N1B—N2B	1.399(4)	N1—N2	1.391
N2A—C3A	1.310(4)	N2B—C3B	1.311(4)	N2—C3	1.319
C1A—C2A	1.435(5)	C1B—C2B	1.423(5)	C1—C2	1.453
C2A—C3A	1.426(5)	C2B—C3B	1.428(5)	C2—C3	1.435
C2A—C5A	1.426(5)	C2B—C5B	1.434(5)	C2—C5	1.440
Torsion angle	**2A**	Torsion angle	**2B**	Torsion angle	$PMBP^-$
C1A—N1A—C12A—C13A	−56.3(6)	C1B—N1B—C12B—C13B	52.9(6)	C1—N1—C12—C13	0
C1A—C2A—C5A—O2A	14.9(6)	C1B—C2B—C5B—O2B	−21.1(6)	C1—C2—C5—O2	20.0
C3A—C2A—C5A—C6A	11.1(7)	C3B—C2B—C5B—C6B	−21.4(7)	C3—C2—C5—C6	26.5
C2A—C5A—C6A—C7A	63.5(6)	C2B—C5B—C6B—C7B	−53.3(6)	C2—C5—C6—C7	49.6

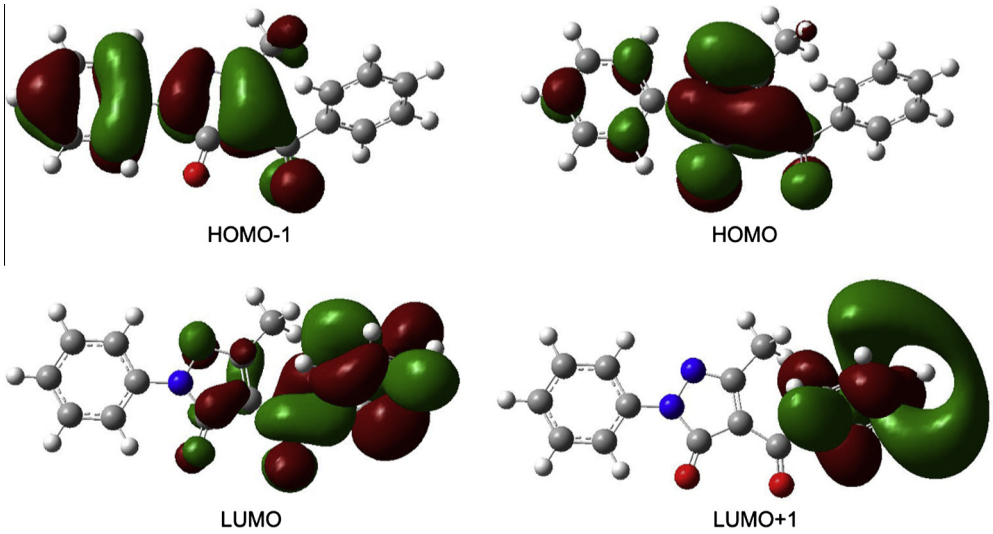

Fig. 5. View of the frontier molecular orbitals of the optimized $PMBP^-$.

acceptors of hydrogen bonds, through which the supermolecular structure is assembled.

The energies and components of molecular orbitals are important characteristics in theoretical studies, which can predict the chemical properties. View of the frontier molecular orbitals of the optimized $PMBP^-$ are shown in Fig. 5. Analysis of the frontier molecular orbital components shows that they distribute nearly evenly on $PMBP^-$. The phenyl rings consisting of C12 ~ C17 and C6 ~ C11 atoms are designated as ring 3 and ring 4, respectively. The HOMO-1 and HOMO orbitals are distributed mainly on the pyrazolone ring and ring 3, while the LUMO and LUMO + 1 orbitals are distributed mainly on ring 4. As the π orbitals of the pyrazolone ring and ring 3 contribute most to the HOMO-1 and HOMO orbitals, the π electrons are delocalized over a large conjugated system built of pyrazolone ring and ring 3. The HOMO orbital is mainly consisted of the *p* orbitals of O1 and O2, and the π orbital of the pyrazolone ring. Thus, O1, O2 and N3 should be more prone to donate electrons into both coordination and hydrogen bonds. However, the large steric hindrance of N3 will hinder the formation of coordination having little impact on hydrogen bonding due to longer interatomic distances. This is also consistent to the experimental result that O1 and O2 chelate with potassium to form compound **1**, and O1, O2 and N2 serve as the proton acceptor of the hydrogen bonds to assemble compound **2**.

Conclusions

A coordination polymer $[K_2(PMBP)_2(H_2O)_3]_n{\cdot}2nH_2O$ and a supermolecule $C_6H_{11}NH_3^+{\cdot}PMBP^-$ were synthesized and characterized by IR, ^1H NMR, elemental analysis, and X-ray crystallography. For compound **1**, each oxygen atoms in the β-diketone coordinates two potassium cations, forming a chain structure. Adjacent chain structures are connected by five-membered water chains involving coordinated and solvent water molecules into three-dimensional network. Compound **2** is a diketonate salt with an organic base where the $PMBP^-$ anions are stabilized by hydrogen bonding, π–π stacking interactions and Van der Waals forces, rather than by coordination to a metal centre. Comparison of the $PMBP^-$ anions between compounds **1**, compound **2** and the optimized one indicates that both coordination and intermolecular weak interactions enables rotation of phenyl rings along the connecting bonds to different degrees. The rotation of the phenyl ring connected with the N atoms disturbs the π electron conjugation with the pyrazolone ring. Coplanarity of the two O atoms in $PMBP^-$ depends on their coordination environment. The calculated MEP maps and frontier molecular orbitals of $PMBP^-$ indicate that O1, O2 and N3 atoms are expected to take part in coordination and hydrogen bonding. But due to the steric hindrance, only oxygen atoms are involved in coordination, which is consistent to the experimental results.

Acknowledgements

This research was supported by the Specialized Research Fund for the Doctoral Program of Higher Education of China (Grant No. 20120132110015), the National Natural Science Foundation of China (Grant Nos. 21371161, 21071134 and 20971115), the Special Foundation for Young Teachers of Ocean University of China (Grant No. 201113025) and the Natural Science Foundation of Shandong Province (Grant No. ZR2012BQ026).

Appendix A. Supplementary material

Selected bond lengths and angles for compounds **1** and **2** are available in the supplementary materials. Additional materials available from the Cambridge Crystallographic Data Centre, CCDC Nos. 923255 (**1**) and 956910 (**2**), contains the supplementary crystallographic data for this paper. These data can be obtained free of charge *via* http://www.ccdc.cam.ac.uk/conts/retrieving.html (or from the Cambridge Crystallographic Data Centre, 12, Union Road, Cambridge CB2 1EZ, UK; fax: +44 1223 336033). Supplementary data associated with this article can be found, in the online version, at http://dx.doi.org/10.1016/j.molstruc.2014.06.057.

References

[1] J.L. Wang, Y. Yang, X. Zhang, F.M. Miao, Acta Cryst. E59 (2003) o430–o432.
[2] S. Umetani, K. Sasayama, M. Matsui, Anal. Chim. Acta 134 (1982) 327–331.
[3] Y. Akama, A. Tong, S. Ishima, M. Kajitani, Anal. Sci. 8 (1992) 41–44.
[4] Y. Akama, T. Nakai, F. Kawamura, Analyst 106 (1981) 250–253.
[5] Y. Akama, T. Nakai, F. Kawamura, Bunseki Kagaku 25 (1976) 496–500.
[6] B.A. Omotow, M.A. Mesubi, Appl. Organomet. Chem. 11 (1997) 1–10.
[7] E.C. Okafor, Spectrochim. Acta 37A (1981) 945–950.
[8] Y. Akama, M. Shiro, T. Ueda, M. Kajitanim, Acta Cryst. C51 (1995) 1310–1314.
[9] Y. Akama, A. Tong, Microchem. J. 53 (1996) 34–41.
[10] F. Bonati, Polyhedron 4 (1985) 357–364.
[11] J.C. Lü, K.L. Yong, J.S. Chen, C.S. Liang, Q.D. Su, Appl. Organomet. Chem. 11 (1997) 1–10.
[12] B.V. Patel, B.T. Thaker, Synth. React. Inorg. Met.-Org. Chem. 16 (1986) 1319–1335.
[13] D. Konozo, M. Yasui, L.S. King, P. Agre, J. Clin. Invest. 109 (2002) 1395–1399.

[14] B. Roux, R. MacKinnon, Science 285 (1999) 100–102.
[15] U. Buck, F. Huisken, Chem. Rev. 100 (2000) 3863–3890.
[16] D.J. Zhou, Q. Lia, C.H. Huang, G.Q. Yao, S. Umetani, M. Matsui, L.M. Ying, A.C. Yu, X.S. Zhao, Polyhedron 16 (1997) 1381–1389.
[17] J. Rebek Jr., Angew. Chem. Int. Ed. 29 (1990) 245–255.
[18] D.B. Amabilino, J.F. Stoddart, Chem. Rev. 95 (1995) 2715–2828.
[19] M.C.T. Fyfe, J.F. Stoddart, Acc. Chem. Res. 30 (1997) 393–401.
[20] A. Harada, J. Li, M. Kamachi, Nature 356 (1992) 325–327.
[21] A. Harada, K. Li, M. Kamachi, Nature 370 (1994) 126–128.
[22] G.M. Whitesides, J.P. Mathias, C.T. Seto, Science 254 (1991) 1312–1319.
[23] M. Albrecht, Naturwissenschaften 94 (2007) 951–966.
[24] SMART and SAINT, Area Detector Control and Integration Software, Siemens Analytical X-ray Systems, Inc., Madison, WI, 1996.
[25] Bruker AXS, SAINT Software Reference Manual, Madison, WI, 1998.
[26] G.M. Sheldrick, Acta Cryst. A64 (2008) 112–122.
[27] K.D. Frisch, G.W. Trucks, H.B. Schlegel, M.A. Robb, J.R. Cheeseman, V.G. Zakrzewski, J.A. Montgomery, Gaussian03, Revision A. 6, Gaussian Inc, Pittsburgh, PA, 2003.
[28] R. Dennington II, T. Keith, J. Millam, GaussView, Version 5.0.9, Semichem Inc, Shawnee Mission, KS, 2008.
[29] J. Emsley, N.J. Freeman, R.J. Parker, H.M. Dawes, M.B. Hursthouse, J. Chem. Soc., Perkin Trans. 1 (1986) 471–473.
[30] O.D. Gupta, B. Twamley, J.M. Shreeve, J. Fluorine Chem. 127 (2006) 263–269.
[31] D. Neculai, A.M. Neculai, H.W. Roesky, J. Magull, G. Bunkòczi, J. Fluorine Chem. 118 (2002) 131–134.
[32] L. Huang, S.B. Turnipseed, R.C. Haltiwanger, R.M. Barkley, R.E. Sievers, Inorg. Chem. 33 (1994) 798–803.
[33] N. Okulik, A.H. Jubert, Internet Electron. J. Mol. Des. 4 (2005) 17–30.
[34] P. Politzer, P.R. Laurence, K. Jayasuriya, J. McKinney, Environ. Health Perspect. 61 (1985) 191–202.